Acoustic models of fish: The Atlantic cod (*Gadus morhua*)

Clarence S. Clay
Department of Geology and Geophysics, University of Wisconsin—Madison, 1215 W. Dayton Street, Madison, Wisconsin 53706

John K. Horne
Ocean Sciences Centre Memorial University of Newfoundland, St. John's, Newfoundland A1C 5S7, Canada

(Received 12 October 1993; accepted for publication 25 March 1994)

Acoustic fish models should represent the fish body form. The Atlantic cod were used to model the acoustic scattering function of teleost fish. The model provides a basis for choices of sonar carrier frequencies. Anesthetized live Atlantic cod ranging from 156 to 380 mm (SL) were "soft" x-rayed to image inflated swimbladders and skeletal elements. Maximum body heights and widths were 0.18 and 0.13 of fish lengths. Lengths and diameters of swimbladder were approximately 0.25 and 0.05 of the fish lengths. A series of short-length fluid-filled cylinders were used to represent body flesh. For carrier frequencies above the breathing mode resonance, swimbladders were modeled as a series of short gas-filled volume elements of cylinders. A Kirchhoff-ray approximation was used to compute the high-frequency acoustic scattering. A low mode solution for a gas-filled cylinder was used to compute the low-frequency "breathing mode resonance." All contributions were added coherently. The scattering lengths $\mathscr{L}$, or target strength $=20\log|\mathscr{L}/L_0|$ (where L_0 is reference length) were sensitive to fish orientation relative to the sonar beam. Theoretical target strengths were compared to the 38-kHz cod data. Agreement was good.

PACS numbers: 43.30.Ft, 43.30.Gv, 43.30.Xm, 43.30.Sf

LIST OF SYMBOLS

a	radius of a cylinder, m. Can have subscripts
A_{sb}	empirical factor in Kirchhoff approximation (10)
c	wave velocity, m/s. Subscripts identify the medium
dB	decibel, 20 log(ratio of pressures, voltages, etc.) or 10 log(ratio of intensities). Logarithm base 10 or 10 log(ratio of intensities). Logarithm base 10
dS	element of area in Helmholtz–Kirchhoff integral, m^2
e	base of natural logarithms, 2.71828...
f	frequency, Hz (hertz or cycles per second). Subscripts give specific frequencies
f_c	carrier frequency, s^{-1}
g	$=\rho_2/\rho_1$, from medium 1 to 2
h	$=c_2/c_1$
i	$=\sqrt{-1}$ imaginary number
j	index number
k	wave number, m^{-1}, $k=\omega/c$. Subscripts give the medium
L	length of a cylinder or fish length, m
L_e	equivalent length of a cylinder m
L_0	reference length, 1 m
$\mathscr{L}$	(spectral) scattering length or amplitude, m
$\mathscr{L}_{bs}$	backscattering length, m
p (...)	acoustic pressure, lower case for time dependence $p(t)$. Subscripts give name, inc for incident, s for scattered, etc.
Q	quality of a resonant system, $Q=f_c/\Delta f$, $Q=1/\delta$
R	range in spherical coordinates, R, θ, and ϕ, m. Subscripts give the application
R_0	reference distance, usually 1 m
$\mathscr{R}_{12}$	plane-wave reflection coefficient at the 1–2 interface
s	rms roughness of surface, m
t	time, s. Subscripts give particular times
$\mathscr{T}_{12}$	plane-wave transmission coefficient at the 1–2 interface. $\mathscr{T}_{12}\mathscr{T}_{21}=1-\mathscr{R}_{12}^2$
TS	target strength, dB. $\mathrm{TS}=20\log_{10}\lvert\mathscr{L}_{bs}/L_0\rvert$ $=10\log_{10}[\sigma_{bs}/L_0^2]$ Reduced TS target strength, $\mathrm{TS}=20\log_{10}\lvert\mathscr{L}_{bs}/L\rvert=10\log_{10}[\sigma_{bs}/L^2]$
u,v,w	coordinates in rotated rectangular system at angle θ (4–7), m. Subscripts give application
x,y,z	coordinates in x,y,z rectangular system, m. Subscripts give application
δ	damping factor, $\delta=1/Q$
Δ	a finite increment as in Δf for a narrow frequency band $\Delta=kL\sin\theta$ in scattering from cylinders
λ	wavelength, m
Δu_j	length of a volume element in rotated coordinates, m
ρ	density, kg/m^3. Subscripts identify the medium
σ_{bc}	backscattering or differential cross section, m^2 $\sigma_{bc}=\lvert\mathscr{L}\rvert^2$
θ	polar coordinate in spherical coordinates angle of incidence in plane-wave reflections, usually with subscripts
ψ_b	empirical phase shift for a soft cylinder in ray-Kirchhoff (10)
ψ_p	empirical phase shift for a fluid cylinder in ray-Kirchhoff (12)
ω	angular frequency, radians/second, $\omega=2\pi f$

 0001-4966/94/96(3)/1661/8/$6.00

INTRODUCTION

Acoustic models of marine organisms form the basis of population and biomass quantitative estimates. Translation of acoustic measurements to the location and size distributions of fish and zooplankton combine acoustic models and statistical descriptions of target scattering processes in sonar beams. It is imperative that acoustic models accurately represent the body form of the modeled organism.

Atlantic cod (*Gadus morhua*) have a single-chambered, physoclistous swimbladder (i.e., not connected to the throat) that occupies 4%–5% of the fish volume.[1–3] This gas-filled organ provides a large acoustic contrast relative to flesh and skeletal elements and is the major source of scattered sound in cod.[4] At long wavelengths relative to the diameter of a fish, the scattering cross sections of flesh and skeletal elements are much lower than scattering cross section of the gas-filled organ because the gas-filled organ has a low-frequency resonance. Over the whole frequency range, most of the scattered sound comes from this gas-filled organ.

Controlled acoustic measurements of scattering functions with freely swimming fish are notoriously difficult to get. Targets are measured under natural conditions but species and length distributions must be verified. Knowledge of the species, sizes, and fish orientations is mostly based on net captures and limited observations.[5–6] Laboratory measurements of tethered live and sometimes dead fish give backscattering measurements of known targets in contrived environments.[7–10] Since the swimbladder is the major source of scattered sound, physiological changes in swimbladders due to movement from holding tanks to depth, anesthetic, or mortality potentially affect laboratory backscattering measurements.

Numerical simulations are a viable alternative. Foote has shown that numerical integrations of acoustic scattering by models of the swimbladders match sound scattering experiments.[11] As an extension, numerical simulations of the sound scattered by acoustic models of fish can be used to determine a good range of sonar carrier or ping frequencies. The acoustic models are constructed to match the anatomy and lengths of the fish. Since we want to use scattering measurements and inversion methods to determine the distribution of fish sizes, the sonar frequencies must be properly chosen. There are practical constraints for sonars that are mounted on the hull or towed over the side of vessels. Low-frequency sonars have large transducers and sound absorption in water gives an upper limit. Commonly sonar carrier or ping frequencies range from 10 to 500 kHz.

We use many of the concepts of Foote's study on scattering of sound in pollock (*Pollachius pollachius*) and saith (*Pollachius virens*).[11] Foote constructed a numerical facet model of the swimbladder's three 3-dimensional surface. He then made a numerical evaluation of the Helmholtz–Kirchhoff integral to compute the scattered sound. The theoretical scattered-sound matched scattering measurements of tethered fish in the L/λ range of 8 to 36, where L is fish length and λ is the acoustic wavelength. Later, Foote and Traynor used a 38-kHz dual beam and split beam sonars to make *in situ* measurements of the target strengths of walleye pollack.[6] Animals were selected from trawl catches for the construction of numerical swimbladder models. Their theoretical sound scattering calculations matched the experimental data. Other acoustic models of fish that use simple geometric bodies are in Refs. 12–15.

TABLE I. Atlantic cod (*Gadus morhua*) Standard lengths, weights, x-ray voltages, and exposures.

Fish	Length (mm)	Weight (g)	Voltage (kV)	Exposure (mA s)
A	173	48	35	38
B	156	34	35	38
C	323	286	40	38
D	380	544	40	38

I. FISH IMAGES

Laboratory held Atlantic cod were anesthesized in a bath saturated with carbon dioxide. The fish were placed on a lead-lined tray and over layers of unexposed Gevaert D-7 Structrix film and wax paper and then radiographed using a General Electric LC-90 x-ray machine. Sizes and x-ray exposures are listed in Table I. Soft x-ray images of fish in Fig. 1 show the flesh, skeletal elements, and the swimbladder. The gas-filled swimbladder has a dark image because air absorbs the x rays less than flesh. Apparently the fish twisted some for the top x rays and the tail sections are wider than the actual fish. The x-ray images were traced and then projected to a standard length using the vertebral column as a ruler between the ventral and lateral views. Visually the proportions of the fish drawings are quite similar, Fig. 2. The reference x axis is along the fish. "Acoustic cod models" were constructed for each fish and then were scaled or extrapolated to larger and smaller lengths for comparison to measurements of cod target strengths. The angles of the swimbladder relative to the x axis are shown. The younger fish, cods A and B, have larger tilts than the older fish C and D.

II. SOUND SCATTERED BY THE ACOUSTIC MODEL

An object is insonified by a plane incident sound wave and the scattered sound pressure is measured at range R from the object. The scattered sound pressure is

$$p_{\text{scat}}(t,R)=(P_{\text{inc}}/R)e^{i(kR-2\pi ft)}\mathcal{L}, \tag{1}$$

where P_{inc} is the amplitude of the incident plane at the object and $\mathcal{L}$ is the scattering length of the object. Note: the acoustic scattering literature also uses the terminology "scattering function $\mathcal{L}(ka)$," "scattering amplitude $S(ka)$," and "form function f_∞" to describe the scattering length that appears in (1).[14–19] Since the function $\mathcal{L}$ has the unit of length we call it "scattering length." The scattering length is dependent on the frequency f or the wave number $k=2\pi/\lambda$ and the orientation of the object relative to the sonar beam. When needed for clarity, the functional dependencies of $\mathcal{L}$ are $\mathcal{L}(ka)$, $\mathcal{L}(L/\lambda)$, and $\mathcal{L}(f)$. The absolute square of the scattering length is the differential or backscattering cross section[16]

$$\sigma_{\text{bs}}=|\mathcal{L}|^2. \tag{2}$$

The target strength TS is

FIG. 1. Ventral and lateral x rays of live Atlantic cod (*Gadus morhua*) Top and side views of cod C (L=323 mm) and cod D (L=380 mm) are shown. The swimbladder is dark; L is standard length.

$$\mathrm{TS}=20\ \log_{10}[|f|/L_0], \tag{3}$$

where L_0 is the reference length, usually 1 m.

There are many ways to calculate scattering lengths. Furusawa used prolate spheroidal models.[12] Do and Surti[13] used elements of cylinders and cones to construct solutions that are based on integrations of the Helmholtz–Kirchhoff integral.[20] In our calculations, the integrations over spheroidal shapes, bent cylinders, etc., are replaced by a summation of the sound scattered from simple elements such as short cylinders and modified cylinders.

The acoustic model fish and the incident wavefront are shown in Fig. 3. In backscattering measurements, the incident plane wave has the angle θ and the sound is scattered back to a transducer in the same direction. The body of the fish has the coordinates, relative to the x axis: $x_b(j)$, $z_{bU}(j)$, $z_{bL}(j)$, and $w_b(j)/2$. Similarly, the swimbladder has the coordinates: $x_s(j)$, $z_{sU}(j)$, $z_{sL}(j)$, and $w_s(j)/2$. In evaluations of the Helmholtz–Kirchhoff integral, the area elements are the projection of the area element on the object onto a reference plane parallel to the incident plane wave. The phases are measured relative to the reference plane. Letting x and z stand for all coordinates, we transform the x-z fish coordinates to the u-v rotated system, Fig. 3(d), using

$$u(j)=x(j)\sin\theta-z(j)\cos\theta, \tag{4}$$

$$v(j)=x(j)\cos\theta+z(j)\sin\theta, \tag{5}$$

$$\Delta u_j=[x(j+1)-x(j)]\sin\theta, \tag{6}$$

$$a_j=[w(j)+w(j+1)]/4, \tag{7}$$

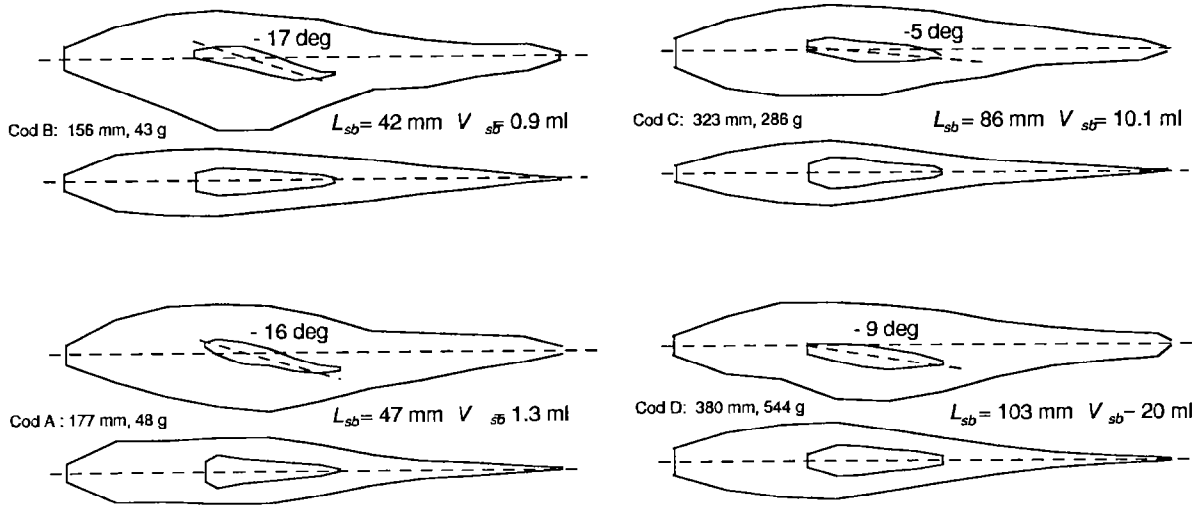

FIG. 2. Schematic diagrams of Atlantic cod (*Gadus morhua*) (A)–(D) showing outlines of body form and swimbladder. Lateral and ventral views are projected to standard lengths for comparisons. Each model drawing has the caudal lengths, swimbladder lengths, swimbladder volumes, and masses of the fish. Angle depressions of the swimbladders are shown. Readers can add their own mouth, eye, and fins.

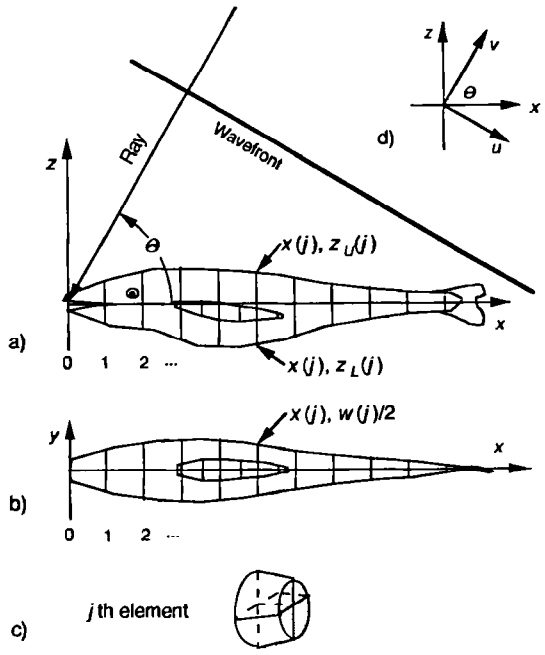

FIG. 3. Geometric construction of acoustic fish models. Cod D is used for the example. Outlines of the fish body and swimbladder, Fig. 2, were digitized at a set of $x(j)$ along the axis of the fish. The upper and lower coordinates are $x(j)$, $z_U(j)$ and $z_L(j)$ and $w(j)$ is the width of the body. The jth volume element is between $x(j)$ and $x(j+1)$. The swimbladder is sampled at smaller spacings. The ray path from the source and its normal, the wavefront, define the directions of the u-v coordinate system. Coordinate u is parallel to the incident wavefront and v is parallel to the incident ray. (a) The ray is incident at the angle θ in the x-z plane. (b) Top view. (c) The swimbladder is omitted from the volume element for clarity. (d) Rotation of x-z to u-v coordinates.

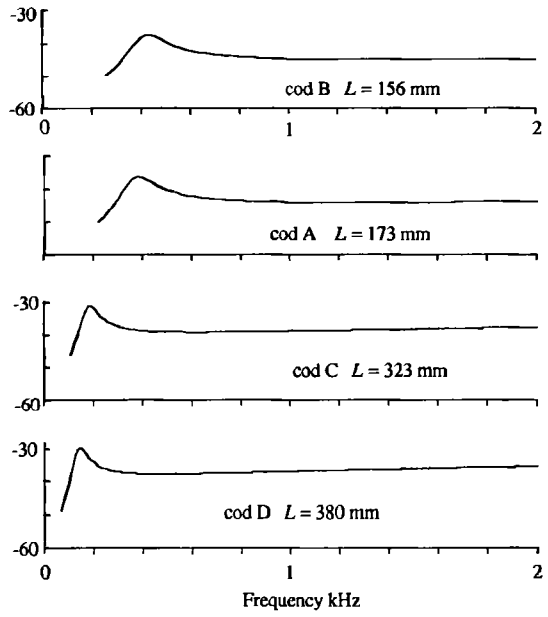

FIG. 4. Target strengths in dB for models of Atlantic cod (*Gadus morhua*). The low-frequency resonance range is shown. TS$=20\log|\mathcal{S}(f)/L_0|$ and $\theta=90$ deg, where $L_0=1$ m. The parameters are in Table II and the fish are at just beneath the water surface. The broad peak is the swimbladder resonance. Numerical expressions in Refs. 16 and 17 were used.

where Δu_j is the projection of Δx along the reference x axis onto u. Generally the scattering theory is limited to angles near $\pi/2$. Choosing a limit of $\sin\theta>0.9$ to specify the nearness, θ can range from 65° to 115°.

A. Low-frequency scattering by the swimbladder

Methods for computing the sound scattered by a finite gas-filled cylinder are in Refs. 14 and 15. The gas-filled cylinder satisfies the boundary conditions for an infinite cylinder. The resonance frequency depends on the radius of the cylinder. It is an approximation for finite length cylinders because boundary conditions at the ends are ignored.[17] The ends of the finite cylinder may be important at very low frequencies. Spherical bubbles satisfy the boundary conditions for spheres,[16,12–25] but spheres do not have the shapes of swimbladders. For a *very-low-frequency* finite length cylinder approximation, we construct an equivalent cylinder by computing the volume of the swimbladder, then use its length to compute the radius of the equivalent cylinder a_e. Thus the unsatisfied boundary conditions are limited to the two ends of the equivalent cylinder. Numerical studies of the mode solutions have shown that the mode solution and Kirchhoff approximation are nearly the same for $ka_e>0.15$. The first cylindrical mode was used to compute scattering amplitudes for $ka_e<0.15$. Thus the swimbladder was approximated as a finite length cylinder for the low-frequency resonance or breathing mode. Details of the resonance calculations are in Refs. 14 and 15. First mode calculations for the cod are shown in Fig. 4. The fish are assumed to be just beneath the water surface or at depth 0. The Q's of the resonance peaks range from 1.8 to 3. These very low values of Q are consistent with measurements.[21,23,25–27]

B. Rather high-frequency scattering: Kirchhoff-ray approximation

1. Swimbladder

The Kirchhoff-ray approximations for the scattering of sound by finite length cylinders are used for high frequencies.[14,15,20] The scattering geometry of a fish is sketched in Fig. 3. From Clay, Eq. (13),[15] the scattering length of a gas-filled (soft) cylinder in water is, with the correction of a missing L_e,

$$\text{soft } \mathcal{S}_K(ka)\approx\frac{L_e}{2\sqrt{\pi}}[(ka+\psi_a)\sin\theta]^{1/2}\frac{\sin\Delta}{\Delta}\times\mathcal{R}_{wc}e^{-i(2ka\sin\theta+\psi_p+\pi/2)},$$

where ψ_a and ψ_p are empirical amplitude and phase adjustments for small ka and the finite cylinder phase factor ($\xi+\pi/4$) is replaced by $-\pi/2$. For a swimbladder in a fish body, we revised the empirical expressions and included the transmission through the fish body to the swimbladder and back out $\mathcal{T}_{wb}\mathcal{T}_{bw}$. The revised expression for the scattering length is

$$\text{soft } \mathcal{S}_K\approx\frac{L_eA_{sb}}{2\sqrt{\pi}}[(k_ba_s+1)\sin\theta]^{1/2}\frac{\sin\Delta}{\Delta}\times\mathcal{T}_{wb}\mathcal{T}_{bw}\mathcal{R}_{bc}e^{-i(2k_ba_s\sin\theta+\psi_p+\pi/2)},$$

$$\Delta=k_bL_e\cos\theta,\quad k_b=2\pi f/c_b, \tag{8}$$

TABLE II. Acoustic parameters.

Medium	ρ kg/m^3	c m/s	$g=\rho_2/\rho_1$	$h=c_2/c_1$
Water $\|_w$	1030	1490	...	...
Fish flesh $\|_b$	1070	1570	1.04	1.05
Swimbladder $\|_c$	1.24	345	0.001	0.22

$$\mathscr{R}_{bc}=\frac{g'h'-1}{g'h'+1}, \tag{9}$$

$$g'=\rho_c/\rho_b \quad \text{and} \quad h'=c_c/c_b,$$

$$A_{sb}\approx\frac{ka_s}{ka_s+0.083} \quad \text{and} \quad \psi_p\approx\frac{ka_s}{40+ka_s}-1.05, \tag{10}$$

where f is frequency; a_s is radius of the cylinder (swimbladder); L_e is the effective length of the cylinder; θ is the angle measured from the axis of the cylinder (or fish) to the incident ray; ρ_b and c_b are the density and sound speed in the fish body; ρ_c and c_c are the density and sound speed in the gas-filled cylinder; $\mathscr{R}_{bc}$ is the reflection coefficient at the fish body–cylinder interface; A_{sb}, (ka_s+1) and Ψ_p are empirical amplitude and phase adjustments for small ka_s; note, $e^{i\pi/2}=-i$.

Typical acoustic parameters for water and fish are given in Table II. The reflection coefficients that are calculated for a gas-filled cylinder in the fish body or in water are nearly the same because $\rho_c/\rho_b\approx\rho_c/\rho_w$ and $c_c/c_b\approx c_c/c_w$. Expression (8) is accurate for $ka_s>0.15$.

The next step uses short sections of modified cylinders as elements of a construction. The transformed coordinates (4)–(6) are used in constructing the summation. The element of scattering length is obtained from (8) by letting L_e become Δu_j in the rotated coordinates. The factor $\sin\Delta/\Delta$, is approximately 1 because $k_bL_e\cos\theta$ is small. The sum of the elements is

$$\text{soft } \mathscr{f}\approx -i\frac{\mathscr{R}_{bc}(1-\mathscr{R}_{wb}^2)}{2\sqrt{\pi}}\sum_0^{N_s-1}A_{sb}$$

$$\times[(k_ba_j+1)\sin\theta]^{1/2}e^{-i(2k_bv_j+\psi_p)}\Delta u_j, \tag{11}$$

$$a_j\equiv[w_s(j)+w_s(j+1)]/4, \tag{12}$$

$$v_j=[v_{sU}(j)+v_{sU}(j+1)]/2, \tag{13}$$

and $k_b\approx k$ at low contrast.

As shown in Fig. 3, the number of terms, $N_s=8$ for the swimbladder summation and, later, $N_b=11$ for the fish body summation was chosen to give an acceptable model of the fish. The model does not give unwarranted details. In our numerical evaluations, we use the coordinates of the middle of each volume element u_j and include a correction for the tapers of z_U, z_L and v_j and w_j from one end of the volume element to the other, Fig. 3(c).

2. Fish body

A ray path construction for the fluid-filled fish body is shown in Fig. 5(a). Somewhat unconventionally, the fish cross section is modeled as a half cylinder over a straight

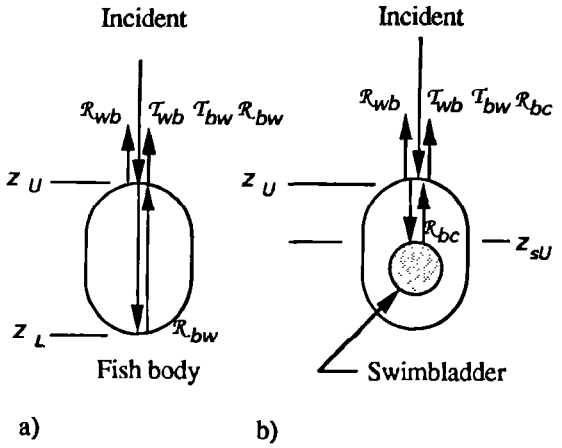

FIG. 5. Ray path constructions. (a) Fish body: Reflection at the upper surface, transmission through the body, reflection at the lower surface, transmission up through the body. (b) Fish body and swimbladder: Reflection from upper surface of the fish body, transmission through the body and reflection at the upper surface of the swimbladder, and transmission from the swimbladder through the body. The transmission coefficient from fish body to inside the swimbladder is very small and reflection paths that pass through the swimbladder to the bottom and back up are negligible.

section over a cylindrical bottom. In Kirchhoff approximation, the top cylinder gives the scattering of the sound wave from the top and the bottom surface gives the scattering from the bottom. The sides make no contributions to the Helmholtz–Kirchhoff integral, however the travel distance adds to the time delay of the reflection from the bottom of the model. The Kirchhoff approximation and construction for low-contrast fluid cylinders are[28]

$$\text{fluid } \mathscr{f}_B\approx -i\frac{L_e}{2\sqrt{\pi}}[(ka\sin\theta)]^{1/2}\frac{\sin\Delta}{\Delta}\mathscr{R}_{wb}[e^{-i2kz_U}$$

$$-\mathscr{T}_{wb}\mathscr{T}_{bw}e^{i2kz_U+i2k_b(z_U-z_L)+i\psi_b}], \tag{14}$$

$$k=\frac{2\pi f}{c_w}, \quad \mathscr{R}_{wb}=\frac{\rho_bc_b-\rho_wc_w}{\rho_bc_b+\rho_wc_w},$$

and

$$\mathscr{T}_{wb}\mathscr{T}_{bw}=1-\mathscr{R}_{wb}^2, \tag{15}$$

$$\psi_b=-\frac{\pi k_bz_U}{2(k_bz_U+0.4)},$$

where z_U and z_L are the upper and lower surfaces of the cylinder; the density and sound speed in water are ρ_w and c_w; a or $w/2$ is the radius as viewed from the top; Ψ_b is an empirical phase correction.

The sum over fluid elements of volume follows from (11)

$$\text{fluid } \mathscr{f}\approx -i\frac{\mathscr{R}_{wb}}{2\sqrt{\pi}}\sum_0^{N_s-1}(ka_j)^{1/2}\Delta u_j[e^{-i2kv_{Uj}}$$

$$-\mathscr{T}_{wb}\mathscr{T}_{bw}e^{-i2kv_{Uj}+i2k_b(v_{Uj}-v_{Lj})+i\psi_b}]. \tag{16}$$

The number of terms, N_b is chosen to give an acceptable model of the fish. The transformed coordinates of the fluid

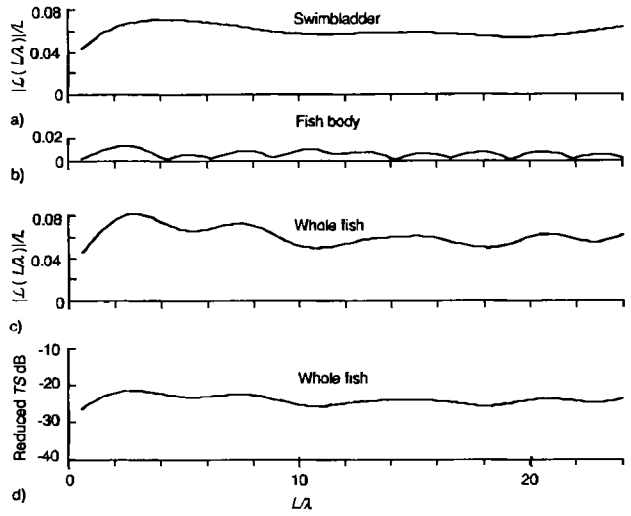

FIG. 6. Reduced scattering lengths for an acoustic model of Atlantic cod (*Gadus morhua*). The acoustic model is cod D ($L=380$ mm, Fig. 2). Modeling parameters are in Table II. (a) $|\mathcal{S}(L/\lambda)|/L$ for swimbladder, (b) fish body, (c) whole fish, and (d) reduced target strengths for whole fish in dB.

body are computed by using expressions similar to (12) and (13).

3. Whole fish

The ray path construction for a swimbladder in the fish body is shown in Fig. 5(b). The real and imaginary parts of the scattering amplitudes from the fish body and swimbladder are added coherently:

$$\mathcal{S}=\text{soft } \mathcal{S}+\text{fluid } \mathcal{S}. \tag{17}$$

The scattering length is a function of frequency f or $\lambda=c/f$, ka and L. The *reduced scattering length*

$$\text{reduced scattering length}=\mathcal{S}(L/\lambda)/L \tag{18}$$

combines these variables into one expression.

Simple generalizations follow: Changes of a fish's structure along the body[29] can be included by moving the reflection coefficients inside of the summation and then letting $\mathcal{R}_{wb}(j)$ and $\mathcal{R}_{bc}(j)$ be the reflection coefficients of the jth element. The "bumpiness" of a swimbladder surface changes the reflection coefficient to $\mathcal{R}_{wc}(j)\exp[-(ks)^2]$, where s is the rms roughness of the surface.[30] The same method can be applied to a bumpy swimbladder.

III. EXAMPLES

Examples of reduced scattering length calculations for cod D are shown in Fig. 6. The incident rays are at 90 deg. The swimbladder scattering, Fig. 6(a) was computed using (11). The fish body, Fig. 6(b), was computed using (16). The whole fish is the coherent sum of the scattering from the swimbladder and the fish body (17). Reduced target strengths for the whole fish are plotted in Fig. 6(d):

$$\text{Reduced TS}=20\log|\mathcal{S}(L/\lambda)/L|. \tag{19}$$

The scattering lengths have strong dependencies on θ. Figure 7 shows the θ dependence for cod D as a function of L/λ. The swimbladder is almost perpendicular to the incident ray at 80°. The smallest value of sin θ is 0.94 for this range of angles. The oscillatory modulations of $|\mathcal{S}(L/\lambda)/L|$ are the contributions of the fish bodies. Choosing $L/\lambda=12$ for an example, the reduced scattering lengths range from 0.01 to 0.1 or 20 dB in target strengths. Clearly, repeated measurements of a fish at different orientations in the sonar beam will give a distribution of echo amplitudes. A Rician probability density function would be expected. Comparisons of target strengths in dB for the models of Atlantic cod are

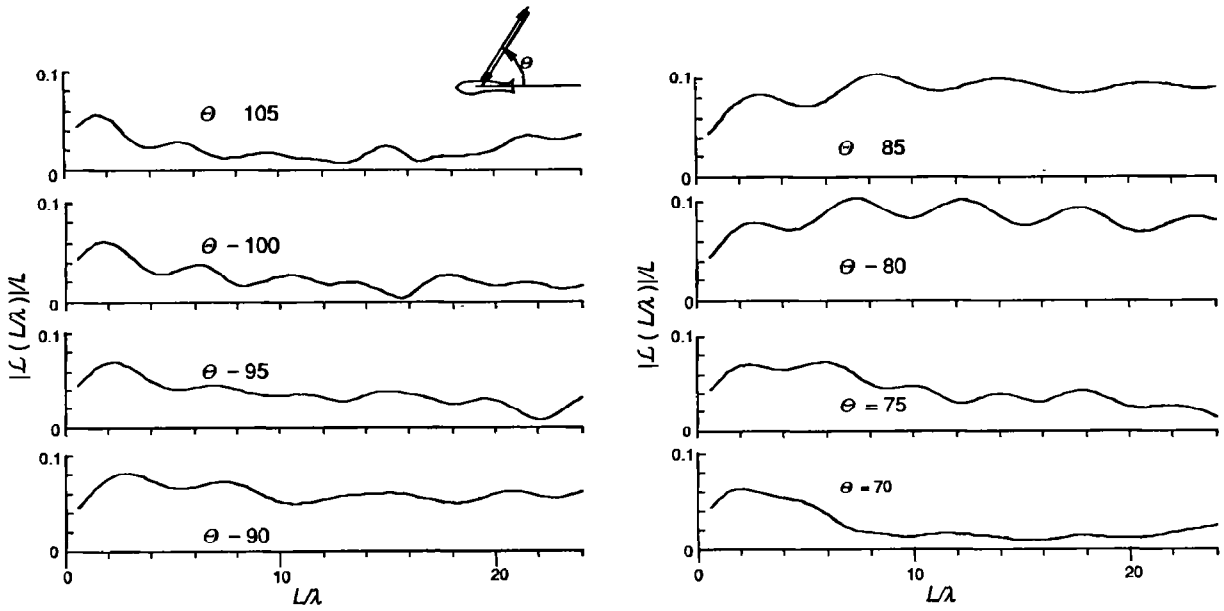

FIG. 7. Dependence of reduced scattering lengths $|\mathcal{S}(L/\lambda)|/L$ on θ The acoustic fish model is cod D ($L=380$ mm). The parameters are in Table II. From Fig. 2, the swimbladder is depressed approximately 9° below the x axis of the fish Since $\theta=81°$ is normal to the axis of the swimbladder, $|\mathcal{S}(L/\lambda)|/L$ is expected to be large for $\theta=80°$. The very-low-frequency resonance responses, Fig. 4, are not shown in this figure.

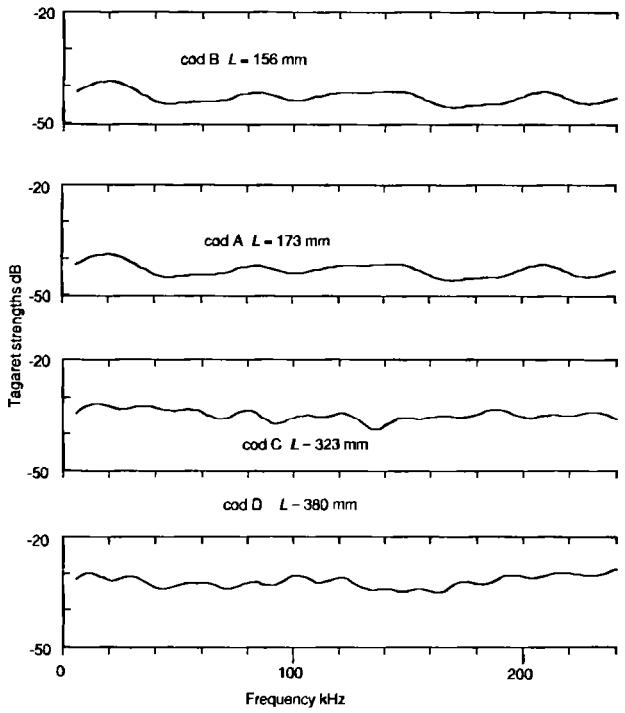

FIG. 8. Target strengths in dB for models of Atlantic cod (*Gadus morhua*). The high-frequency range is shown. TS=20 $\log|\mathcal{F}(f)/L_0|$ and θ=90 deg, where L_0=1 m.

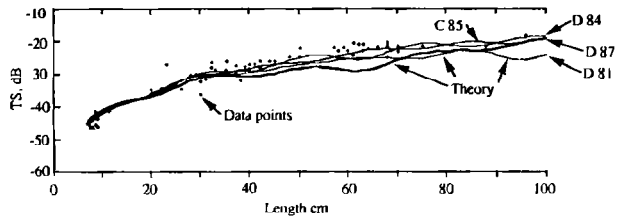

FIG. 9. Comparison of target strengths from the acoustic models at 38 kHz and data. The data points (+) are the maximum target strength measurements of Nakken and Olsen for Atlantic cod (*Gadus morhua*).[10] Their measurements of tethered fish were made at 38 kHz and fish lengths varied from 8 to 96 cm. Fish orientations were adjusted for maximum TS. C 85 means theoretical or model curve for cod C at θ=85°. D 84 means theoretical or model curve for cod D at θ=84°, etc. The maxima of the model curves are to be compared to the data.

shown in Fig. 8. The incident rays are at 90° to the fish axis in this figure. The maximum L/λ of cod B is about 25 and the maximum L/λ is about 60 for cod D. Recalling Fig. 6, we expect the sensitivity to orientation to be large.

IV. COMPARISONS TO DATA

The programs for numerical computations of the scattering lengths were written and the scattering length calculations were made prior to comparisons to experimental measurements. Ideally, live fish should be used for measurements because the swimbladder is an active organ in fish. Echoes from live fish have a Rician probability density function.[31,32] Usually it is necessary to use captured fish so that the species and sizes are known. To control fish orientation, fish are often tethered from a frame. The same laboratory and experimenters are likely to report consistent data. Since our acoustical model is sensitive to the fish structure, we wanted use measurements of a single cod over a wide range of frequencies or measurements of many lengths of fish at a single frequency. From the literature we chose the 38-kHz scattering data for cod that were taken by Nakken and Olsen.[10] Nakken and Olsen's careful sonar measurements met all criteria except the first. They used mortally wounded or dead fish. They made extensive measurements of the dependence of the target strength on the orientation angle. Their Fig. 40 gives the dependence of target strengths on fish lengths. The data are the *maximum measured target strength* for any orientation angle. Since the fish were dead, choices of the maxima bias the results toward larger target strengths relative to the mean-square scattering lengths from live fish. Points for the 38-kHz data were read from their figure. Figure 9 compares the Nakken and Olsen data and the acoustic model calculations. Computations are shown for cod C at 85 deg and cod D at several angles. Since the data are the maximum target strengths, the envelope of the maxima of the acoustic model calculations should be compared to the data. The longest fish was cod D, 38 cm. All computations for longer fish are extrapolations of cod D as a representative body form. Cod C, 32.3 cm appears to match the data a little better. The extrapolations down to 8 cm are good.

V. CONCLUSIONS

Acoustic model calculations match 38-kHz laboratory measurements over the fish length range of 8 to 95 cm. The scattering amplitudes depend on fish orientation relative to the direction of the sonar beam. Figure 7 shows the sensitivity of $\mathcal{F}$ to the orientation angles. Choosing for an example L/λ=12, the values of $\mathcal{F}(L/\lambda)/L$ range from about 0.1 to 1, or about 20 dB.

Sonar beamwidths and the directional scattering of fish enter into sonar measurements. Suppose the sonar has a 2° full beam width and is vertical. If all of the fish are "well behaved" and have their axis horizontal, the scattering amplitude will be about 0.5 at L/λ=12. Similarly, for a wide beam sonar that has 20° full beam width, the scattering amplitudes would range from 0.1 to 1 or 20 dB. Measurements of target strengths and volume scattering that are made using a very narrow beam sonars are likely to be biased toward smaller target strengths. Presumably one can use multiple beam sonars to determine the directional dependence of the scattering amplitudes.

Four observations: (1) The resonance regions for all of the fish were below 1 kHz, Fig. 4. This region is below the usual operating range of standard pinging sonars. Because of the width of the peak, explosive sources are commonly used for measurements in this frequency range.[26,27]

(2) Inversion methods use scattering measurements that are made at multiple frequencies. Solutions depend on the scattering lengths having a sequence of "definitive" maxima and minima.[33]

The inversion task for fish is more difficult than for zooplankton because the swimbladder extends the scattering response down to low frequencies and $L/\lambda \approx 0.2$ and the scattering length as a function of frequency has less "character. Referring to Fig. 7, the scattering lengths at L/λ=2 are about

the same at all angles of tilt. The scattering lengths are dependent of the tilt for $L/\lambda = 4$, 6, 8, and 10 and measurements at these frequencies of L/λ would give the tilt of the fish.

(3) For identifying fish, a set of frequencies in the L/λ range of 2 to 10 are likely to be more useful for inversion than data taken at larger L/λ ratios.

(4) If one picks a value of L/λ in Fig. 7, then the set of scattering lengths for all angles of incidence has many values. We believe that a large set of numerical simulations for many angles, as in Clay and Heist, would give a Rician PDF of echo amplitudes.[31]

ACKNOWLEDGMENTS

Work supported by the National Science Foundation (OCE-8817171) Office of Naval Research (N-00014-89-J-1515, M. Blizzard) (CSC). The Natural Science and Engineering Council of Canada, the Ocean Production Enhancement Network, and National Centres of Excellence—Canada (JKH). We thank K. Clark, D. Methven, and P. Pepin for supplying the cod. C. George and T. Shears assisted with the x rays. Contribution number 554 Geophysical and Polar Research Center, University of Wisconsin (CSC). Contribution number 239 the Memorial University of Newfoundland (JKH). We also thank the associate editor, J. H. Miller, and the two reviewers.

[1] O. Sand and A. D. Hawkins, "Measurements of swim-bladder volume and pressure in cod." Norw. J. Zool. **22**, 31–34 (1974).

[2] F. R. Harden Jones and F. Scholes, "Gas secretion and resorption in the swimbladder of the cod *Gadus morhua*," J. Comp. Physiol. B **135**, 319–331 (1985).

[3] P. J. P. Whitehead and J. H. S. Blaxter, "Swimbladder form in cludpoid fishes," Zool. J. Linn. Soc. **97**, 299–372 (1964).

[4] K. G. Foote, "Importance of the swimbladder in acoustic scattering by fish: a comparison of gadoid and mackerel target strengths," J. Acoust. Soc. Am. **67**, 2084–2089 (1980).

[5] L. G. Rudstam, C. S. Clay, and J. J. Magnuson, "Density estimates and size of cisco, Coregonus artedii, using analysis of echo peak PDF from a single transducer sonar," Can. J. Fish. Aquat. Sci. **44**, 811–821 (1987).

[6] K. G. Foote and J. J. Traynor, "Comparisons of wall eye pollock target strength estimated determined from *in situ* measurements and calculations based on swimbladder form," J. Acoust. Soc. Am. **83**, 9–17 (1988).

[7] R. W. G. Haslett, "Determination of the acoustic backscattering patterns and cross sections of fish," Br. J. Appl. Phys. **13**, 349–357 (1962).

[8] R. W. G. Haslett, "Determination of the acoustic scatter patterns and cross sections of fish models and ellipsoids," Br. J. Appl. Phys. **13**, 611–620 (1962).

[9] R. H. Love, "Dorsal-aspect target strength of an individual fish," J. Acoust. Soc. Am. **49**, 816–823 (1971).

[10] O. Nakken and K. Olsen, "Target strength measurements of fish," Rapp. P.-V. Reun. Cons. Int. Explor. Mer. **170**, 52–69 (1977).

[11] K. G. Foote, "Rather-high-frequency sound scattered by swimbladdered fish," J. Acoust. Soc. Am. **78**, 688–700 (1985).

[12] M. Furusawa, "Prolate spheroidal models for predicting general trends of fish target strength," J. Acoust. Soc. Jpn. **9**, 13–24 (1988). Note: Furusawa used a vacuum filled spheroid for the swimbladder.

[13] M. A. Do and A. M. Surti, "Estimation of dorsal aspect target strength of deep-water fish using a simple model of swimbladder back scattering," J. Acoust. Soc. Am. **87**, 1588–1596 (1990).

[14] C. S. Clay, "Low-resolution acoustic scattering models: Fluid-filled cylinders and fish with swim bladders," J. Acoust. Soc. Am. **89**, 2168–2179 (1991). Note: Figs. 12 and 13 plot reduced scattering amplitudes.

[15] C. S. Clay, "Composite ray-mode approximations for backscattered sound from gas-filled cylinders and swimbladders," J. Acoust. Soc. Am. **92**, 2173–2180 (1992).

[16] C. S. Clay and H. Medwin, *Acoustical Oceanography* (Wiley, New York, 1977)

[17] T. K. Stanton, "Sound scattering by cylinders of finite length. I. Fluid cylinders," J. Acoust. Soc. Am. **83**, 55–63 (1988).

[18] T. K. Stanton, "Sound scattering by cylinders of finite length. III. Deformed cylinders," J. Acoust. Soc. Am. **86**, 691–705 (1988).

[19] W. G. Neubauer, *Acoustic Reflection from Surfaces and Shapes* (Naval Research Laboratory, Washington, DC, 1986). Gives a summary of scattering research at Catholic University in H. Überall's group and the group at Naval Research Laboratory. Has many careful experiments.

[20] G. C. Gaunaurd, "Sonar cross sections of bodies partially insonified by finite sound beams," IEEE J. Ocean. Eng. **OE-10**(3), 213–230 (1985).

[21] I. B. Andreeva, "Scattering of sound by air bladders of fish in deep sound scattering ocean layers," Sov. Phys. Acoust. **10**, 17–20 (1964).

[22] W. E. Batzler and G. V. Pickwell, "Resonant acoustic scattering from gas bladder fish," in *Proceedings of an International Symposium on Biological Sound Scattering in the Ocean*, edited by G. B. Farquhar (U.S. Govt. Printing Office, Washington, DC, 1970).

[23] B. S. McCartney and A. R. Stubbs, "Measurement of the target strength of fish in dorsal aspect, including swimbladder resonance," pp. 180–211 in *Proceedings of an International Symposium on Biological Sound Scattering in the Ocean*, edited by G. B. Farquhar (U.S. Govt. Printing Office, Washington, DC, 1970).

[24] R. H. Love, "Resonant acoustic scattering by swimbladder-bearing fish," J. Acoust Soc. Am. **64**, 571–580 (1978).

[25] A. Løvik, and J. M. Hovem, "An experimental investigation of swimbladder resonance in fishes," J. Acoust. Soc. Am. **68**, 850–854 (1979).

[26] D. V. Holliday, "Resonance structure in echoes from schooled pelagic fish," J. Acoust Soc. Am. **51**, 1322–1332 (1972).

[27] T. Akal, R. K. Dullea, G. Guidi, and J. H. Stockhausen, "Low-frequency volume reverberation measurements," J. Acoust. Soc. Am. **93**, 2535–2548 (1993).

[28] T. K. Stanton, C. S. Clay, and D. Chu, "Ray representation of sound scattering by weakly scattering deformed fluid cylinders: Simple physics and applications to zooplankton," J. Acoust. Soc. Am. **94**, 3454–3462 (1993).

[29] Y. Sun, R. Nash, and C. S. Clay, "Acoustic measurements of the anatomy of fish at 220 kHz," J. Acoust Soc. Am. **78**, 1772–1776 (1985).

[30] T. K. Stanton and D. Chu, "Sound scattering by rough elongated elastic objects. II: Fluctuations of scattered field." J. Acoust Soc. Am. **92**, 1665–1678 (1992).

[31] C. S. Clay and B. G. Heist, "Acoustic scattering by fish acoustic models and a two-parameter fit," J. Acoust. Soc. Am. **75**, 1077–1083 (1984).

[32] K. G. Foote, A. Aglen, and O. Nakken, "Measurement of fish target strength with a split-beam echo sounder," J. Acoust Soc. Am. **80**, 612–621 (1986).

[33] D. V. Holliday, R. E. Pieper, and G. S. Klepple, "Determination of zooplankton size and distribution with multifrequency acoustic technology," J. Cons. Int. Explor. Mer. **46**, 52–61 (1989).